

Combining measurements and modeling/simulations analysis to assess carbon nanotube memory cell characteristics

J. Farmer, D. Veksler, E. Tang, G. Bersuker
MTD, The Aerospace Corporation
Los Angeles, CA

D. Z. Gao, A.-M. El-Sayed, T. Durrant, A. Shluger*
Nanolayers Research Computing LTD, UK
* UCL, London, UK

T. Rueckes, L. Cleveland, H. Luan, R. Sen
Nantero Inc., Woburn, MA, USA

Abstract— A simulation package for CNT memory cells is developed, based on computational modeling of both the mesoscopic structure of carbon nanotube films and the electrical conductivity of inter-CNT contacts. The developed package enables the modeling of various electrical measurements and identification of a range of operation conditions delivering desirable device characteristics. This approach opens the path for optimization of the CNT fabric to meet performance requirements.

Index Terms— Neuromorphic computing, NVM, RRAM, carbon nanotubes.

I. INTRODUCTION

Carbon nanotube (CNT) fabrics display intrinsic complexity due to their fabrication as randomly oriented and packed nanotubes of variable length, radius and chirality. Electrical conductivity properties of these disordered structures are considered to be defined by resistance of the inter-CNTs contacts [1]. Both contact instability as well as variations in their arrangements induces switching variability and degradation of memory states. This hampers identification of specific material features controlling electrical characteristics and, thus, the ways to improve the fabrication process and optimize operation conditions. Therefore, combining electrical

measurements with modeling of the material structure and simulations of electron transport through the CNT film, Fig. 1, is becoming imperative for reaching performance targets. Here we present the results of simulations based on physics-based modeling of CNT fabrics to determine device electrical properties.

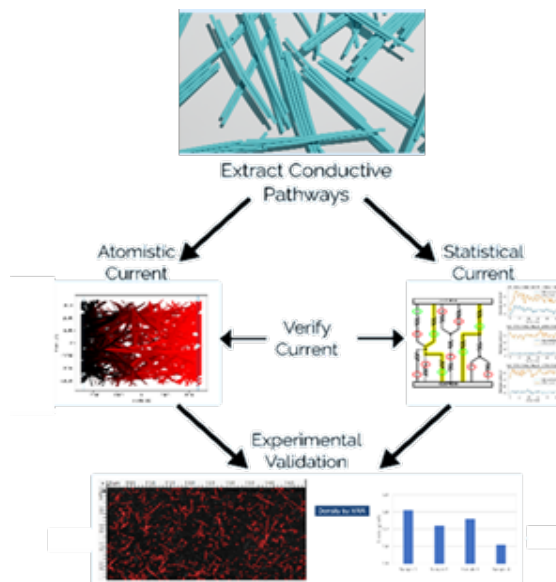


Figure 1. Device technology evaluation scheme: from material modeling to statistical simulations to electrical-physical testing.

II. SIMULATIONS AND MEASUREMENTS

CNT films with dimensions relevant to experimental devices are constructed using a mesoscopic potential [2], where the nanotubes are coarse-grained into connected cylindrical segments are shown in Fig. 2. Parameterized to higher level simulations, mesoscopic description enables to study dynamics of nanotube systems of various dimensions and compositions, accounting for multiple factors such as length, chirality and fabric density.

Two major factors affecting the tubes mutual arrangement are their bending energy and van der Waals (vdW) interaction. Due to the attractive vdW forces, the total energy is lowered when tubes are closely adjacent to each other, as occurs during the film densification. This vdW interaction facilitates formation of CNT bundles, like those seen in Fig. 2. and Fig. 3. They deform to maintain the minimum vdW separation of 0.3 nm. Bundle size depends on the tube length, with shorter CNTs tending to form bundles with a significantly larger number of tubes. Bundles can contact their neighbors; their mutual orientations determine sizes/types of the electrical contacts formed.

In order to produce high-density CNT films with particular relevance to the CNT fabrics employed in memory cells, a two-stage process was used to construct the mesoscopic models. An initial film structure was generated by distributing the individual CNTs randomly in space. Secondly, a densification process was performed where a force was applied to the top of the CNT film in order to compress it and to increase its density. This densification process is shown schematically in Fig. 2. As a result of this compression, the CNTs formed discrete bundles in order to improve their packing. Using this process, films with a density of $\sim 0.6 \text{ g/cm}^3$ were produced.

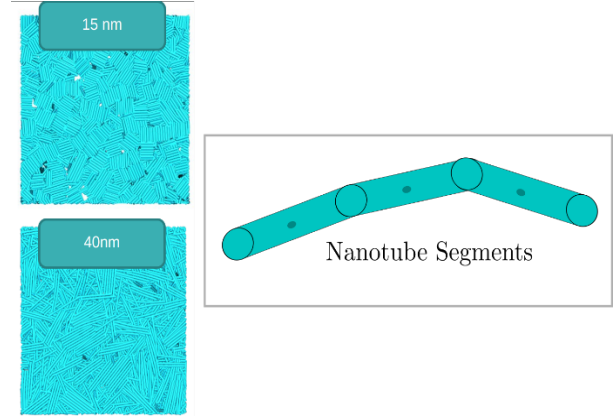


Figure 2. Example of the mesoscopic model calculations of a structure of 15 nm and 40 nm CNT films. Breaking down nanotubes into segments allows reproducing their elasticity and intra-tubes bending.

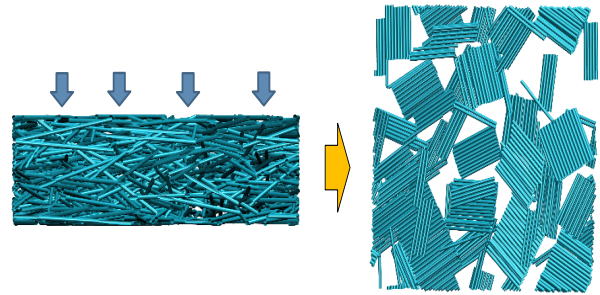


Figure 3. As the initial structure shown on the left is compressed, it becomes denser and the formation of bundles is enhanced. A fully densified structure is shown on the right, demonstrating enhanced bundle formation.

Once these structures are generated, the electrical conductivity are investigated using the characteristics of CNT-to-CNT junctions calculated using atomistic simulations. Density functional tight binding (DFTB) was used to simulate the contacts [3]. Then, the electrical conductivity was evaluated using the non-equilibrium Green's function (NEGF) approach. Some example structures are shown in Fig. 4. In order to make the junction structures more realistic, many random structural perturbations were applied in order to explore the range of available conductivities in the disordered fabrics generated using the mesoscopic model.

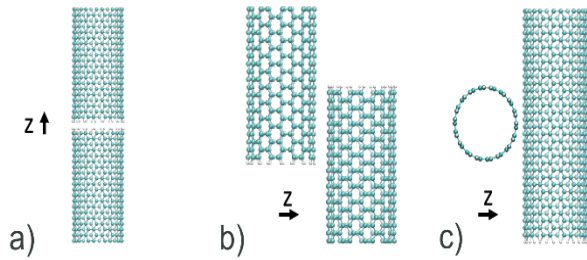


Figure 4. Example CNT contact structures employed in the calculation of CNT-CNT contact electrical conductivity via DFTB+NEGF technique. a) Tip-to-top structure demonstrating low electrical conductivity. b) wall-to-wall structure demonstrating high electrical conductivity c) perpendicular configuration displaying intermediate conductivity.

Taken together, the performed mesoscopic and atomistic calculations demonstrate two main features of the CNT fabrics: (1) bundled CNTs are strongly coupled and require significant energy in order to separate. Additionally, a large surface area of contacts enables effective (low resistance) electron tunnel between CNTs (2) Contacts between CNTs in different bundles have a smaller area. Hence, less energy is required to modify such inter-tubes contacts, which exhibit greater resistance due to lower electron tunneling. Hence, it is reasonable to expect that the electrical switching in such CNT fabrics is dominated by the type (2) contact discussed here. These insights is taken forward to model device performance.

In simulating memory operation processes, one must consider that in resistive non-volatile memories (NVM) the current is determined by structural features supporting electron transport [4]. Atomic-level structural changes are driven by local heating determined by dissipated energy E , which is controlled by the magnitude of the current through a given conductive path at a given moment in time, $I(t)$. Larger amount of energy released under longer programming time ($t + \Delta t$) may induce additional structural changes that can further modify current (either to higher $>$ or lower $<$ magnitude): $I(t + \Delta t)$ $I(t)$: longer time \rightarrow higher released energy \rightarrow more structural changes \rightarrow greater chance for modifications affecting electron transport. Thus, the NVM cell characteristics are strongly affected by operation time duration. For this reason, device

assessment should be performed under the test conditions which are close to actual circuitry operations [5 - 7]. Indeed, measurements collected using the ultra-short pulse setup, Fig. 7, demonstrate that higher released energy caused by the increase of switching pulse duration from 1 ns to 2 ns induces significant structural changes, as demonstrated by a drastic reduction/collapse of the memory window, Fig. 8. These additional structural changes happen to result in more resistive HRS related to larger CNTs separations due to deeper vdW minima: consequently, the system got stuck in HR manifested by memory window collapse.

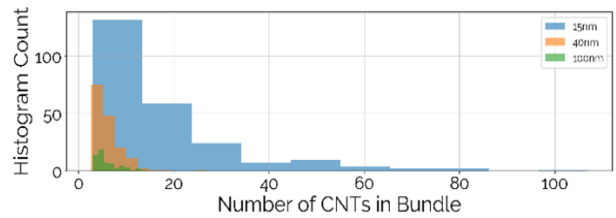


Figure 5. Bundles size dependency on CNT lengths. Shorter tubes form larger bundles. Note similar size distributions for 40 and 100 nm CNT lengths.

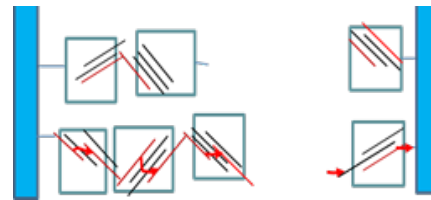


Figure 6. Schematics of conductive paths between top-bottom electrodes formed by randomly oriented bundles with variable numbers of CNTs.

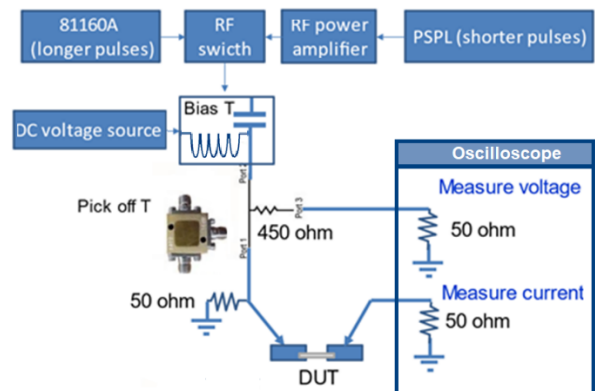


Figure 7. Experimental setup of the ultra-short pulse test.

The developed Python simulation package (NRAMPY) accounts for the aforementioned temperature variations induced by local current flows. Using material modeling data, Figs. 2, 5, 9c, NRAMPY constructs a unique one-bit cell, which is represented by numerous conductive paths formed by chains of contacting bundles between the top and bottom electrodes, Fig. 6. Each path consists of several bundles, both fixed and changeable (switchable) intra-bundle contacts and Schottky contacts between the bundles chain and metal electrodes. Simulations employ statistical distribution of the physical parameters defining the cell conductivity, such as area density of conductive paths, number of bundles in each path, CNT compositions in bundles, % of types of inter-bundles CNT contacts, etc., Fig. 9 a,b. Bundle sizes are extracted from a Poisson distribution, linear resistance values are determined as the contributions of CNT overlaps and intrinsic resistances of each CNT. Intra-bundle contact resistance is taken from ballpark conductivity values based on atomic-level calculations, Fig. 9c.

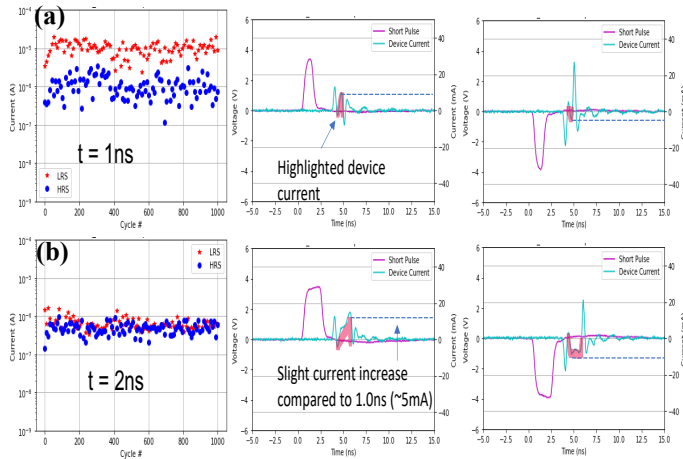
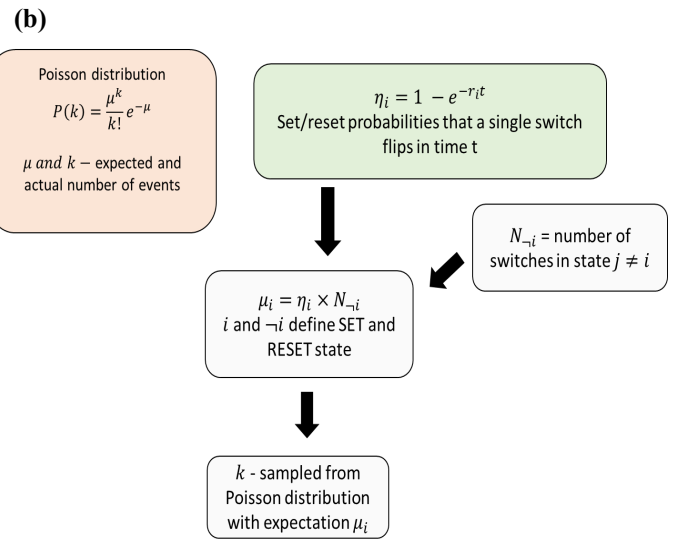
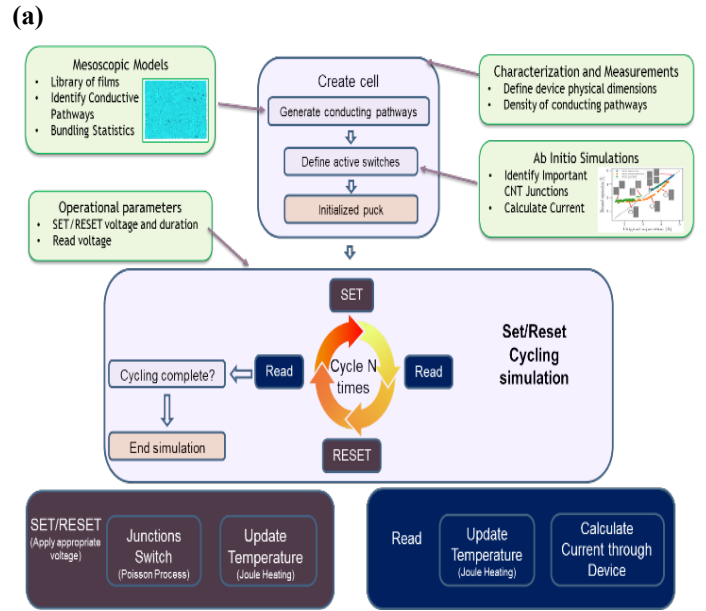


Figure 8. Cycling with (a) 1 ns and (b) 2 ns pulse durations and associated Set and Reset I-V characteristics. Red curve is an applied pulse voltage, blue curve is the associated current through the cell, artificially shifted wrt voltage curve along x-axis to make its shape visible. Red-marked areas outline the pulse-induced cell current. The size of this area is proportional to the magnitude of released energy. Current peaks adjacent to the marked areas (both ahead and behind) are the displacement currents induced by fast voltage transients.



Junction type	Subtype	Maximum current (μA)	Minimum current (μA)	Minimum resistance ($\text{k}\Omega$)	Maximum resistance ($\text{k}\Omega$)
CNT intrinsic	-	77.5	-	6.5	-
Intra-Bundle contact	20 nm CNTs	18.9	9.45	26.5	52.9
	40 nm CNTs	37.7	18.9	13.3	26.5
	60 nm CNTs	56.7	28.4	8.8	17.6
Non-bundled contact	Parallel b)	2.2	0.02	227	25000
	Perpendicular c)	0.4	0.004	1250	125000
	Tip-to-tip a)	0.003	0.00003	16666	16666667

Figure 9. (a) Simulation software NRAMPY: architecture, operational sequence and input variables. (b) Calculation sequence for Set/Reset operations. Variables in simulation program: number of conductive paths; number of bundles in each conductive path; number of CNTs controlling conductance across in- and out- sites in each bundle; % of different CNT contact types between bundles; % of switching contacts in each conductive path. (c) Current/resistance

across a bundle with two CNTs of 20nm, 40nm, 60nm lengths and between contacting non-bundled CNTs from DFTB+NEGF calculations.

Switching simulations were performed within a range of operational voltages and pulse durations of interest and compared to electrical measurements, as shown in Figs. 10 and 11. Simulations and measurements match well, though the measured data exhibit higher variability, indicating that certain physical processes are not yet accounted for and will be addressed in a follow-up study.

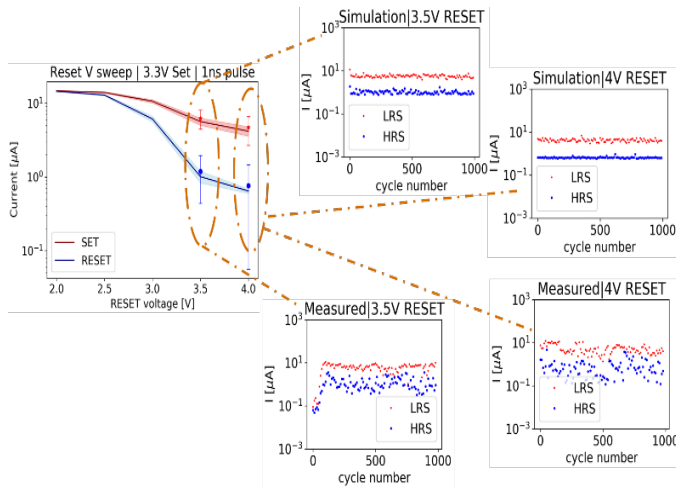


Figure 10. Example of 1 ns pulse switching simulation over a range of Reset voltages and a fixed Set V= 3.3V and corresponding measurements.

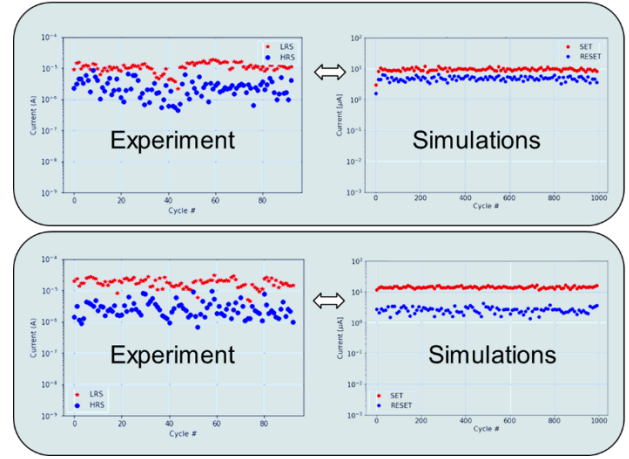


Figure 11. Measurements-simulations comparison of 3.5V Set/4V Reset switching cycles with 0.5ns and 1ns pulse durations.

III. SUMMARY

By combining experimental measurements with material modeling results we developed a practically useful simulation package, which reproduces main features of the NVM electrical characteristics in a wide range of circuitry-relevant operation conditions down to sub-nanosecond duration. It allows to identify optimum conditions for a specific device structure, as well as material modifications needed to meet performance requirements.

References:

1. P. Nirmalraj et al, Electrical conductivity in single-walled carbon nanotube networks, J. Am. Chem. Soc. (2005)
2. L. Zhigilei et al, Mesoscopic model for dynamic simulations of carbon nanotubes, Phys. Rev. B (2005)
3. B. Hourahine et al, DFTB+, a software package for efficient approximate density functional theory based atomistic simulations, J. Chem. Phys.
4. G. Bersuker et al, Metal oxide resistive random access memory (RRAM) technology. In: *Advances in Non-volatile Memory and Storage Technology*, Elsevier, 2019.
5. J. Farmer et al, Mitigating switching variability in carbon nanotube memristors, IRPS (2021)
6. W. Whitehead et al, Overcoming limitations in evaluation of memristor technologies for neural networks, PRIME (2020).
7. F. Zhang et al, An Ultra-fast Multi-level MoTe2-based RRAM, IEDM (2019)